

# PULSE SCANNING SYSTEM OF THE MEDICAL BEAM AND THE SYSTEM OF RECORDING THE POSITION OF THE BEAM AND THE DISTRIBUTION OF AN IRRADIATION DOSE OF THE OBJECT

I. Yudin, A. Makankin, V. Panacik, S. Tyutyunnikov, S. Vasilev, A. Vishnevskiy,  
Joint Institute for Nuclear Research, Dubna, Russia

K. Laktionov, D. Yudin, N.N. Blokhin National Medical Research Center of Oncology,  
Moscow, Russia

## Abstract

This work describes the pulse scanning system of the medical beam and the system of recording the position of the beam and the distribution of the irradiation dose of the object. Our report deals with the construction of the carbon beam transport line for biomedical research at the NICA accelerator complex, JINR, Dubna.

We are discussed the compilation and realization of the plan of treating a tumor located at a depth up to 30 cm. The hardware realization of the beam scanning is shown.

We describe the wire chamber and read out electronics which were developed for on-line monitoring of the "intensive" extracted beams of relativistic nuclei. The system has been tested in several acceleration runs with deuteron beams with the intensity up to  $10^{10}$  1/s and carbon ion beams. The system allows one to make multiple measurements of the two-dimensional beam intensity distribution and beam position during the beam spill.

## THE CHANNEL FOR BIOMEDICAL RESEARCH

One direction in the development of the JINR accelerator complex NICA [1] is the design of a test bench for biomedical research based on the JINR Nuclotron. While designing the test bench, the general technique for manufacturing the hadronic therapy complex is tested.

This channel is intended for the transportation of the  $^{12}\text{C}^{6+}$  carbon ions with an intensity of  $\sim 2 \times 10^9$  and an energy of 100–550 MeV/nucleon. The channel starts near the F3 focus of the primary channel [2].

## Setup Restrictions

The following optical elements are used in the channel: dipole and deflecting magnets (SP-94) and a magnetic lens (ML-17).

The length of the transport channel is 12 m. The designed channel starts from a dipole magnet mounted in the primary transport channel at a distance of 5.25 m in front of the F3 focus of the primary channel. Optical elements (quadrupole lenses) are located over the channel. There is a beam trap at the end of the channel, the test bench in  $F_k$  (focus C, see [2]) is right before the trap, and the beam scanning system is before the test bench. The scanning system consists of two similar deflecting magnets rotating at an angle of  $90^\circ$  around the axis relative each other.

One natural restriction of beam transportation is that the diameter of the vacuum pipeline is equal to 0.25 m, which passes through all the quadrupole elements of the system. A magnet aperture of  $0.3 \times 0.13$  m is a restriction at the final stage of the scanning system. The mutual position of the scan region and the system of scanning magnets is fixed.

The maximum current is limited for each quadrupole lens; this results in a limitation of the coefficient  $K < 1.5 \text{ m}^{-2}$  used for calculating the phase incursion on the lens at a preset energy range of 100–550 MeV/nucleon.

The beam cross section in the F3 focus of the primary transport channel is a circle 0.04 m in diameter, which makes it possible to define the initial conditions of beam propagation.

## Results Obtained

For a preset aperture and the magnet arrangement, we have [2]: 1) a minimum focus diameter of 2.8 mm for an emittance of  $25\pi$  mm mrad; 2) a minimum focus diameter of 5.6 mm for an emittance of  $50\pi$  mm mrad. The region of target scanning is restricted by an aperture of two successive magnets in a plane normal to the beam. The magnet aperture is  $0.3 \times 0.13$  m for a specific channel; this agrees with the planned scan region of  $0.1 \times 0.1$  m. Solutions have been found for emittances of  $25\pi$  mm mrad and  $50\pi$  mm mrad based on the above specified restrictions. The beam cross section in the focus C (see [2]) is close to the minimum for the given scanning system geometry: 1)  $3.0 \times 3.0$  mm for an emittance of  $25\pi$  mm mrad; 2)  $5.6 \times 6.0$  mm for an emittance of  $50\pi$  mm mrad.

We suggest the following equipment for the additional channel: 1) magnetic lenses ML-17; 2) scanning and dipole magnets SP-94; 3) the pixel chamber and the wire chamber and readout electronics.

## MONITORING CHAMBER SYSTEM

Functional test samples of detectors and electronics for them designed for monitoring the Nuclotron ion beam were constructed at LHEP department no. 5: 1) a wire chamber with front-end electronics and detection electronics installed in a data acquisition crate located far from the beam channel and 2) a pixel ionization chamber built with the use of electronics designed at JINR.

This system is designed to perform the following functions: 1) conduct multiple measurements of the ex-

tracted beam profile and the beam position in the  $XY$  plane during the beam dump in a wide range of intensities from  $10^5$  to  $10^{10} \text{ s}^{-1}$ ; 2) determine the overall beam particle flux in the beam dump; 3) measure the distribution of the irradiation dose at the irradiated object in the  $XY$  plane.

### *Two-Coordinate Wire Beam Chambers*

The chamber incorporates two signal planes for recording the projection of the beam intensity distribution onto the  $X$  and  $Y$  axes. The signal anode planes are placed between three high-voltage cathode planes. Each signal plane is basically an array of wires with a diameter of  $25 \text{ }\mu\text{m}$  made from gold-plated tungsten that are arranged with an interval of  $2 \text{ mm}$ . Each signal plane incorporates  $96$  wires. The corresponding active region size is  $192 \times 192 \text{ mm}^2$ . Each wire may be connected to the detection electronics. High-voltage planes are made from stainless grid. The wire diameter is  $50 \text{ }\mu\text{m}$ . The grid cell size is  $0.5 \times 0.5 \text{ mm}^2$ , and the interelectrode gap is  $6.5 \text{ mm}$ . The chambers are constantly purged with a gas mixture based on argon and carbon dioxide with the addition of propanol vapor. When the beam intensity is high, the chambers operate in the regime of collection of the ionization charges produced in the interelectrode gap. When the beam intensity is low, the chambers may operate in the gas multiplication regime at up to  $10^4 \text{ s}^{-1}$ .

**Wire Chamber Electronics.** The wire chamber electronics incorporates the frontend electronics installed at a distance of up to  $1.5 \text{ m}$  from the beam, the ADC unit mounted in the remote data acquisition crate at a distance of no less than  $30 \text{ m}$ , and the so-called sequencer generating a train of control pulses for synchronizing the system operation. The sequencer is also located in the remote crate. A single the frontend electronics board incorporates  $32$  channels for recording the current values from the chamber wires at specific time points. The board is basically a multichannel analog memory element and an analog multiplexer for connecting the memory channels sequentially, one after another, to the remote ADC mounted in the data acquisition crate. Each board has a single analog output that is activated if the channel being triggered is located at this board. If this is not the case, the analog output is disabled. The outputs of all boards may be tied together for readout with a single ADC channel. Each board is addressed with the use of switches located on it. Thus, all the channels tied together for readout with a single ADC channel are lined up in a single queue with consecutive numbering. The boards are mounted in twos in NIM bins (i.e., a single bin incorporates  $64$  channels). In response to a signal from the sequencer, the instantaneous value of the input current is saved simultaneously in all channels of the system incorporating many boards. The channels from the general queue are then sequentially connected to the ADC with the help of a control pulse train.

In accordance with the technical requirements, the decay-time constant of the signal formed in the first

stage was set to be equal to  $330 \text{ }\mu\text{s}$ . This means that we may perform data sampling with a period down to  $1 \text{ ms}$  in order to obtain correct data on the dynamics of changes that the beam is undergoing. The sequencer mounted in the data acquisition crate serves to generate (on command from the crate controller or upon the arrival of an external trigger signal) a pulse train that is needed in order to control the synchronous operation of the frontend electronics and the ADC. The output signals are displayed on the front panel. The sequencer was constructed using  $2\text{K} \times 8$  memory. Prior to the start of operation in the acceleration run, the sequencer requires loading  $2048$  8-bit words, which set the needed configuration of the control pulse train at the output terminals, into the memory through the crate bus. When it is triggered by an external signal or on command through the crate bus, the internal generator produces  $2048$  pulses and stops. The pulse counter generates the address for the sequential readout of 8-bit words. Every bit of each successive word affects the generation of a signal through one of the eight output terminals at the front panel. Calibration dependences for several detection channels incorporating the frontend electronics and the ADC in the data acquisition were obtained with the use of a test current supply. The voltage dependences of the chamber gas amplification for two gas mixtures based on argon and carbon dioxide with the addition of propanol vapor are used. The electronics for pixel chambers (to be discussed below) was used to measure these dependences. The charge passing between the chamber electrodes in unit time upon irradiation with a Sr-90 radioactive source was recorded.

The combination of the gas amplification capacity and the dynamic range of the detection electronics yields a dynamic range of the system of no less than five orders of magnitude.

### *Pixel Ionization Chamber*

The basic design of this chamber is similar to the one of the wire chamber. The cathode is made from a grid of stainless wires with a diameter of  $50 \text{ }\mu\text{m}$ . The cell size is  $0.5 \times 0.5 \text{ mm}^2$ . The anode plane is a removable element of the chamber. A plane made from glass-fiber laminate with a thickness of  $1 \text{ mm}$  was used in the considered case. The active region with an area of  $160 \times 160 \text{ mm}^2$  is divided into  $256$  separate sensitive pads (pixels). Each of them is connected to a terminal at the periphery of the printed board. The pixel size is  $10 \times 10 \text{ mm}^2$ . The interelectrode gap may be varied in a wide range starting from  $6.5 \text{ mm}$  with the use of inserts.

The pixel chamber was purged in beam runs with the same gas mixture (based on argon and carbon dioxide with the addition of propanol vapor) that was used in the case of the wire chamber.

**The pixel chamber electronics** incorporates two unit types: the frontend electronics near the chamber and the data acquisition unit mounted in the data acquisition crate located far from the beam channel.

**The frontend electronics of the pixel chamber** is located up to 1.5 m from it and is based on the TERA06 microcircuit chip produced in Italy [3]. The main features of TERA06 are as follows. Each of the 64 channels converts the input current into pulse rate with continuous counting of the number of pulses by a 16-bit counter. The counter readings may be shifted into the 64-word output register at any specific time on command from the data acquisition unit. The register contents are read out word after word into the data acquisition unit mounted in the crate located far from the beam channel. The counter does not stop at this time. Thus, the system operates without dead time. The quantum of conversion of the input current into frequency is varied with the use of external potentials within the range from 100 to 800 fC. The maximum conversion frequency is 5 mHz. The average noise per channel is on the order of 1 1/s. The frontend unit and the data acquisition unit designed at JINR are used in the described system. With the chosen settings, the quantum of conversion of the input current into frequency is roughly equal to 600 fC. A total of 64 detection channels were used. This corresponded to an active area size of  $80 \times 80 \text{ mm}^2$  in the pixel chamber.

Figures 1 and 2 show examples of visualized data on the distribution of the cumulative dose obtained in real time after each dump of the beam onto the target.

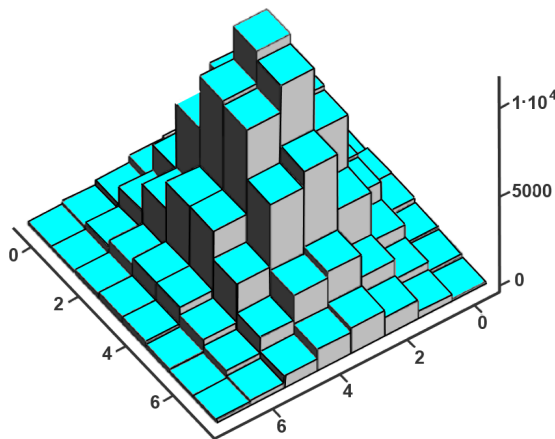


Figure 1: The view of 3D-distribution of beam is for on-line monitoring of the beam.

## CONCLUSIONS

Test samples of the following systems were constructed: 1) two coordinate wire chambers with an active area size of  $192 \times 192 \text{ mm}^2$  and the electronics for them and 2) the pixel ionization chamber with an active area size of  $160 \times 160 \text{ mm}^2$  and 256 pads with a size of  $10 \times 10 \text{ mm}^2$  that is operated with the detection electronics based on the TERA06 microcircuit chip.

The systems ensure the monitoring of the extracted relativistic Nuclotron ion beams in real time and allow one to perform 1) multiple measurements of the beam profile, its center position, and its intensity during the beam dump; 2) measurements of the distribution of

the cumulative target irradiation dose after each dump. The system was tested in a series of Nuclotron acceleration runs (see Fig. 3) at the “QUINTA” setup [4] and performed efficiently at deuteron beam intensities of up to  $10^{10} \text{ 1/s}$  and carbon ion beams.

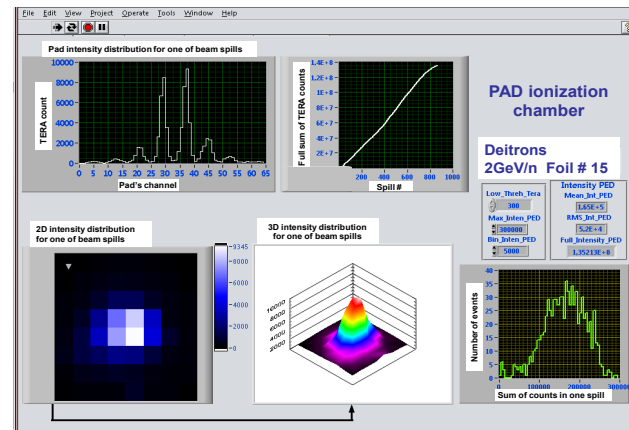


Figure 2: The on-line monitoring of the beam.

The construction of the carbon beam transport line for applied and biomedical research at the Nuclotron accelerator complex, JINR, Dubna is shown. We have studied the scheme and modes of magneto-optical elements of the channel. Used electronics described. We are discussed the compilation and realization of the plan of treating a tumor located at a depth up to 30 cm. Choice of beam scanning schemes and their optimization are shown.

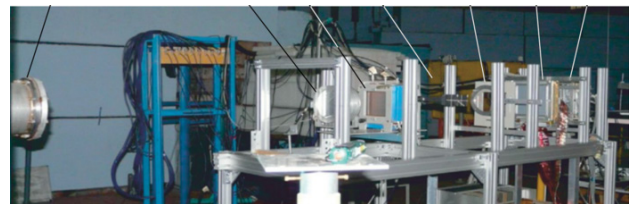


Figure 3: The pixel chamber and the wire chamber in the line at the QUINTA experiment in the 205 building of LHEP JINR.

## REFERENCES

- [1] N. Agapov et al., “NICA project at JINR,” in Proceedings of the XXIII Russian Particle Accelerator Conference, St. Petersburg, Russia, 2012, MOXCH03, pp. 5-8.
- [2] I.P. Yudin, V.A. Panasik, and S.I. Tyutyunnikov An Additional Carbon Ion Transport Channel for Biological Research at the Nuclotron of the Joint Institute for Nuclear Research, Physics of Particles and Nuclei Letters, 2012, Vol. 9, No. 3, pp. 283–287. © Pleiades Publishing, Ltd., 2012. ISSN 1547-4771.
- [3] G. Mazza et al., “A 64-channel wide dynamic range charge measurement ASIC for strip and pixel ionization detectors,” IEEE Trans. Nucl. Sci. **52**, 847–853 (2005).
- [4] A.I. Berlev et al., The Measurement of the Neutron Flux Using Diamond Detector at the “Quinta” Setup. Physics of Particles and Nuclei Letters. 2016. Vol.13. № 3. pp.352-357.